Ministry of Science, Research and Technology
University of Bonab

Mechanics in Nano-Engineering

journal homepage: https://mneng.ubonab.ac.ir/

Mechanics in NANO-ENGINEERING

Numerical thermal management of Li-ion batteries using phase change materials: A transient 2D-axisymmetric study

Maryam Mahmoudi
Alpha Digital Technology, Karaj, Alborz, Iran

ARTICLE INFO

Article history:
Received 9 15 2026
Received in revised form 10 1 2026
Accepted 11 9 2026

Keywords:
Lithium-ion battery
Battery thermal management system
Phase change material
Enthalpy-porosity method
2D-axisymmetric transient modeling
COMSOL Multiphysics

ABSTRACT

Efficient battery thermal management systems (BTMS) are critical for maintaining safe operating temperatures and preventing thermal runaway in lithium-ion batteries. This study presents a rigorous two-dimensional (2D) axisymmetric transient numerical model using the enthalpy-porosity method in COMSOL Multiphysics to evaluate the thermal performance of a phase change material (PCM) sleeve (3–4 mm thickness) encasing an 18650 Li-ion battery. The model comprehensively captures the solid-liquid phase change progression, latent heat absorption, and the transition from conduction-dominated heat transfer to buoyancy-driven natural convection within the PCM domain. The numerical results indicate that an optimized 3–4 mm PCM sleeve effectively regulates the maximum cell temperature below the critical threshold (50 ˚C) under transient high-rate discharge conditions. Furthermore, the analysis elucidates the spatial distribution of the melting front, liquid volume fraction evolution, and local energy flux variations during continuous operation. These findings provide valuable design guidelines for optimizing compact, passive BTMS configurations in cylindrical battery packs, contributing to enhanced thermal safety and extended service life in electric vehicle applications.

1. Introduction

With the rapid expansion of electric vehicles and renewable energy storage systems, lithium-ion (Li-ion) batteries have become the dominant technology in this industry due to their high energy density, favorable lifespan, and low self-discharge rate[1]. However, the performance, safety, and lifespan of these batteries are strongly influenced by their operating temperature. Optimal performance of Li-ion batteries requires maintaining the cell temperature within a safe range (typically between 20°C and 45°C) and achieving a uniform temperature distribution across the cell surface. Operating the battery at temperatures higher than the allowable limit can lead to rapid capacity degradation, a reduction in useful life, and under critical conditions, the occurrence of thermal runaway and explosion. Consequently, comprehensive studies on battery energy storage highlight that advanced thermal management and monitoring strategies are vital for ensuring overall battery safety and long-term reliability[2].

To address these thermal challenges, various battery thermal management systems (BTMS) have been developed. Among active and passive cooling solutions, the utilization of phase change materials (PCM) as a passive cooling method has attracted significant attention due to its high latent heat capacity, which prevents sudden increases in battery temperature without requiring external electrical energy or moving parts. Nevertheless, conventional PCMs suffer from poor thermal conductivity, prompting extensive research into advanced configurations and thermal enhancement techniques[3, 4]. For instance, Hussien et al[5]. demonstrated that optimizing PCM encapsulation geometry and surface-to-volume ratio can significantly enhance melting efficiency and reduce peak battery temperatures during dynamic discharge operations. Similarly, Talele and Zhao[3], investigated nano-enhanced PCMs, showing that dispersing nanoparticles into paraffin wax prevents premature liquidous states and improves overall thermal effectiveness.

To further boost the heat dissipation capabilities of PCM-based systems, researchers have integrated porous media and extended surfaces. Najafi Khaboshan et al[6]. explored the combination of PCM, metal foam, and various fin shapes, reporting substantial temperature reductions and delayed melting fronts. In a related experimental and numerical study, Abhishek et al[7]. evaluated the impact of fin configurations and cell spacing, confirming that passive cooling drastically extends the safe working time of 18650 battery packs compared to natural convection. Furthermore, advanced composites such as nickel and copper foam-paraffin matrices have been experimentally proven to lower surface temperatures significantly while improving thermal uniformity, whereas intelligent thermal regulators utilizing PCM volume changes offer dynamic negative feedback for variable ambient conditions.

It is well-documented that thermal runaway in lithium-ion batteries is primarily driven by exothermic side reactions and the subsequent release of combustible and high-temperature gases from the volatile electrolyte. As internal temperature rises, these generated gases increase cell pressure and alter the internal thermal characteristics. Although the present 2D-axisymmetric model primarily focuses on transient heat conduction and phase change within the PCM jacket, acknowledging the role of gas generation is crucial for understanding the comprehensive failure mechanism of lithium-ion systems.

Despite extensive literature on PCM-enhanced BTMS configurations, a detailed, transient analysis focusing specifically on the continuous evolution of the PCM melting front, solid-liquid phase fraction distribution, and its mutual effect on energy flux in 2D-axisymmetric cylindrical geometries still requires deeper investigation. A precise understanding of transient behaviors and heat transfer mechanisms at the battery-PCM interface is crucial for optimizing cooling layer thicknesses and selecting ideal operational parameters.

In this study, a two-dimensional axisymmetric (2D-axisymmetric) numerical model has been developed to simulate the transient thermal behavior in an 18650 cylindrical battery cell equipped with a PCM cooling jacket. By simultaneously applying heat transfer equations in solids and fluids and modeling the phase change process, the temporal and spatial temperature distribution, PCM melting front, phase fraction, and passing energy flux over a period of 1800 seconds have been evaluated. The results obtained from this numerical simulation provide a precise perspective on passive cooling performance and furnish a practical tool for the optimal design of battery thermal management systems.

To establish a clear scientific context, numerous relevant studies on passive battery thermal management systems and PCM-based cooling strategies are reviewed and critically synthesized below.

The thermal management of lithium-ion batteries has attracted considerable research interest over the past decade, leading to various active and passive cooling methodologies designed to maintain optimal operating temperatures and prevent thermal runaway. In recent years, extensive numerical and experimental investigations have focused on optimizing phase change material (PCM) systems, thermal conductivity enhancers, and geometric configurations to maximize heat dissipation efficiency. A detailed review of these preceding studies reveals the evolution of passive battery thermal management systems (BTMS) as outlined below.

The rapid proliferation of electric vehicles (EVs) and high-power energy storage systems has intensified the need for efficient battery thermal management systems (BTMS) to ensure optimal operating temperatures (**20-45** °C) and prevent thermal runaway in lithium-ion (Li-ion) batteries. Among various passive, active, and hybrid cooling configurations, phase change material (PCM) embedded systems have gained substantial prominence due to their high latent heat capacity, structural simplicity, and autonomous operation without parasitic power consumption[8-12]. However, the inherent low thermal conductivity of conventional PCMs often leads to localized heat accumulation, prompting extensive research into performance enhancement techniques, structural optimizations, and multi-physics numerical modeling[13-15].

Recent advancements in passive BTMS have focused heavily on geometric modifications and fin integration. For instance, Choudhari et al[13]. numerically investigated the thermal performance of PCM modules integrated with various fin shapes (rectangular, triangular, trapezoidal, I-shape, and T-shape) across different discharge rates, demonstrating that optimized fin structures significantly enhance conduction and reduce peak temperatures by up to $\mathbf{9.28}\%$ at a 3C discharge rate. Similarly, Bais et al[14]. analyzed a passive BTMS using RT-42 PCM with varying thicknesses ($\mathbf{1}$-$\mathbf{7}$ mm) on a cylindrical 18650 cell at a 3C discharge rate, concluding that a minimum thickness of $\mathbf{4}$ mm is crucial for effective temperature control, though complete melting was not observed throughout the cycle. While these studies highlight the benefits of fin configurations and layer thickness, they largely rely on localized experimental setups or simplified thermal networks without capturing the detailed continuous transient melting front dynamics.

To address complex multi-physics and system-level integrations, Zhang et al[15]. developed a 3D transient thermal model for an integrated battery-PCM-converter system, revealing that horizontal and vertical thermal conductivities ($\boldsymbol{k_{xy}}$ and $\boldsymbol{k_z}$) exert distinct effects on delay time and surface temperature uniformity. Concurrently, Shravan Kumar and Prasad Rao[7], provided a comprehensive review on composite phase change materials (CPCMs) incorporating nano-additives, metal foams, and fins to mitigate thermal runaway risks under realistic EV driving cycles. Expanding upon material optimization, Li et al[9]. conducted a sensitivity analysis of thermophysical parameters, identifying that phase transition temperature has the most pronounced impact on maximum temperature reduction, followed by latent heat and thermal conductivity.

Furthermore, fundamental electrochemical-thermal (EC-HT) coupling approaches have been established to dissect detailed heat generation mechanisms. Eze et al[10]. coupled a 3D electrochemical model with a 2D axisymmetric heat transfer model to compare tabbed and tables cylindrical cell designs, noting that negative current collectors account for over $\mathbf{80}\%$ of total heat at 1C. In a similar methodological direction, Muñoz et al[11]. parametrized and validated an electrochemical P2D model coupled with a 2D axisymmetric thermal framework for commercial cylindrical cells using fast optimization algorithms. Moreover, Ahmadian-Elmi and Zhao[12], emphasized the critical necessity of evaluating PCM latent heat absorption and buoyancy-driven natural convection within cylindrical battery packs, while Kibria et al[16]. systematically reviewed the integration of metal foams, nanometal oxides, and innovative fin configurations to optimize lightweight PCM-BTMS for electric vehicle applications.

Despite these comprehensive contributions, a notable research gap persists. While existing literature extensively explores 3D system-level integrations, complex multi-fin structures, or pure electrochemical P2D interactions, detailed 2D-axisymmetric transient investigations focusing specifically on the continuous solid-liquid phase change progression, latent heat absorption distribution, and local energy flux variations across optimized $\mathbf{3}$-$\mathbf{4}$ mm PCM sleeves for 18650 cells under transient discharge remain underexplored. To bridge this gap, the present study establishes a rigorously validated 2D-axisymmetric transient numerical model using the enthalpy-porosity method in COMSOL Multiphysics, capturing the detailed thermal regulation, melting front dynamics, and spatial energy flux characteristics of the PCM-enhanced battery system.

In parallel with geometric and system-level configurations, understanding the fundamental transient melting dynamics and natural convection within cylindrical geometries is crucial for accurate thermal modeling. Soliman et al[17]. experimentally and numerically investigated PCM melting in cylindrical enclosures under constant heat flux, demonstrating that melting is initially conduction-dominated before transitioning into a buoyant natural convection regime characterized by a curved solid-liquid interface. Expanding on numerical accuracy, Moench and Dittrich[18], emphasized that incorporating buoyancy-driven natural convection flow and volumetric expansion into simulation frameworks—such as advanced modifications within COMSOL Multiphysics—yields significantly higher fidelity compared to simplified conduction-only models.

Furthermore, advanced material enhancements have been extensively explored to overcome the intrinsic thermal transport limitations of conventional PCMs. Daiz et al[19]. demonstrated that embedding nano-encapsulated phase change materials (NEPCMs) within porous cavities significantly improves heat storage and transfer under natural convection, while Ali Basem[20], established that incorporating nanofluids within PCM enclosures accelerates the melting process and reduces phase transition time by up to $\mathbf{5}\%$ at higher concentrations. These insights collectively underscore the importance of integrating rigorous transient natural convection and advanced thermophysical enhancements into numerical frameworks designed for cylindrical energy storage systems.

2. Governing Equations

The mathematical modeling of the transient thermal and hydrodynamic behavior of the 18650 cylindrical lithium-ion battery equipped with a phase change material (PCM) sleeve involves coupled heat transfer, solid-liquid phase change, and fluid flow. The governing equations applied to the different domains are formulated as follows:

2.1. Energy Conservation in the Battery Cell

The transient heat conduction and internal heat generation within the cylindrical battery cell are governed by the energy conservation equation:

$$\rho_b C_{p,b} \frac{\partial T_b}{\partial t} = \nabla \cdot (k_b \nabla T_b) + \dot{q}_{gen} \qquad (1)$$

where ρ_b, $C_{p,b}$, and k_b represent the density, specific heat capacity, and thermal conductivity of the battery cell, respectively. T_b is the battery temperature, t is time, and $\dot{q}_{gen}$ denotes the volumetric heat generation rate within the cell resulting from electrochemical reactions and ohmic polarization.

2.2. Transient Heat Transfer and Phase Change in the PCM Domain

To model the solid-liquid phase change and thermal energy storage within the PCM, the enthalpy-porosity technique is utilized. The transient energy equation incorporating the latent heat of fusion is expressed as:

$$\rho_{pcm} C_{p,pcm} \left(\frac{\partial T_{pcm}}{\partial t} + \mathrm{u} \cdot \nabla T_{pcm} \right) = \nabla \cdot \left(k_{pcm} \nabla T_{pcm} \right) - \rho_{pcm} L \frac{\partial \alpha_m}{\partial t} \qquad (2)$$

where ρ_{pcm}, $C_{p,pcm}$, and k_{pcm} are the density, specific heat, and thermal conductivity of the PCM, respectively. T_{pcm} is the temperature, L is the latent heat of fusion, and u is the velocity vector of the molten PCM.

The liquid fraction (phase fraction), α_m, defines the ratio of melted PCM within a given control volume and is evaluated as:

$$\alpha_m = \begin{cases} 0 & \text{if } T_{pcm} < T_{solid} \\ \dfrac{T_{pcm} - T_{solid}}{T_{liquid} - T_{solid}} & \text{if } T_{solid} \le T_{pcm} \le T_{liquid} \\ 1 & \text{if } T_{pcm} > T_{liquid} \end{cases} \qquad (3)$$

where T_{solid} and T_{liquid} are the solidus and liquidus temperatures of the PCM, respectively.

2.3. Fluid Flow and Hydrodynamics in the Molten PCM Region

During the melting process, natural convection currents arise in the liquid phase of the PCM. The fluid motion is modeled using the continuity and Navier-Stokes equations, coupled with the Bossiness approximation to account for buoyancy-induced density variations:

- Continuity Equation:

$$\nabla \cdot \mathrm{u} = 0 \qquad (4)$$

- Momentum Conservation Equation:

$$\rho_{pcm}\left(\frac{\partial \mathrm{u}}{\partial t} + (\mathrm{u}\cdot\nabla)\mathrm{u}\right) = -\nabla p + \mu_{pcm}\nabla^2\mathrm{u} + \rho_{pcm}\beta\mathrm{g}\left(T_{pcm} - T_{ref}\right) + \mathrm{S} \qquad (5)$$

where p is static pressure, μ_{pcm} is dynamic viscosity, β is the thermal expansion coefficient, g is gravitational acceleration, and T_{ref} is the reference temperature.

2.4. Mushy Zone Treatment (Darcy's Law Source Term)

To suppress fluid velocity and simulate the porous-like behavior in the solid-liquid transition region (mushy zone), the Carman-Kozeny damping approach is incorporated as the momentum source term S:

$$\mathrm{S} = -\frac{C_{amorph}(1-\alpha_m)^2}{\alpha_m^3 + \epsilon}\mathrm{u}$$

where C_{amorph} is the mushy zone morphological constant, and $\epsilon = 10^{-3}$ is a small numerical stabilization parameter to prevent division by zero.

3. Numerical and Analytical Solution Methods

In this section, the numerical implementation framework for simulating the transient thermal behavior and solid-liquid phase change of the 18650 cylindrical batteries equipped with a PCM jacket is presented. First, the governing physics and solver configurations in COMSOL Multiphysics are described. Next, the computational domain, boundary conditions, and the mesh independence study are detailed.

Although real lithium-ion batteries feature a complex, interleaved spiral structure consisting of cathode, anode, and separator layers, modeling every microscopic layer directly introduces prohibitive computational costs. Following well-established methodologies in battery thermal management, a macroscopic homogenized cylindrical approach is adopted in this study. The effective thermophysical properties assigned to the cell domain represent the combined anisotropic or equivalent behavior of these layered components, providing an accurate and efficient prediction of the global thermal response.

3.1. Numerical Implementation and Solver Settings in COMSOL Multiphysics

The coupled multi-physics problem involving transient heat conduction, natural convection, and phase change dynamics within the 2D-axisymmetric battery-PCM system was solved using the finite element method (FEM) via COMSOL Multiphysics. The "Heat Transfer in Solids and Fluids", "Phase Change Material", and "Creeping Flow" interfaces were fully coupled.

To handle the strong nonlinearity introduced by the moving solid-liquid interface, latent heat absorption, and buoyancy-driven convection, a fully coupled solver approach was employed. The PARDISO direct solver was utilized for linear system solutions, ensuring high numerical stability and convergence. A strict relative convergence tolerance of 10^{-4} was set for all dependent variables (temperature, velocity components, and pressure). The time-dependent study was executed over a total operational discharge period of 1800 s with an adaptive time-stepping scheme to precisely capture the transient evolution of the melting front.

3.2. Computational Domain and Boundary Conditions

Due to the cylindrical geometry of the 18650 cell and its concentric PCM sleeve, a two-dimensional axisymmetric coordinate system (r-z) was established, significantly reducing computational cost while maintaining high spatial accuracy.

- Symmetry Axis: A symmetry axis boundary condition ($\frac{\partial}{\partial r} = 0$) was applied along the centerline of the battery cell.
- Outer Boundary of the PCM Sleeve: Convective heat transfer boundary conditions were applied to the outer walls of the PCM jacket exposed to the ambient environment, governed by $-k_{pcm}\nabla T \cdot \mathrm{n} = h_{amb}(T - T_{amb})$, where h_{amb} represents the ambient convective heat transfer coefficient and T_{amb} is the ambient temperature.
- Top and Bottom Boundaries: Standard adiabatic or minor convective heat loss boundary conditions were considered for the end faces of the battery-PCM assembly.
- No-slip Condition: A non-slip boundary condition ($\mathrm{u} = 0$) was enforced for the molten PCM velocity at all solid-fluid interfaces (battery casing and container boundaries).

3.3. Mesh Independence Study

To ensure that the numerical simulation results are independent of the spatial discretization resolution, a rigorous mesh convergence study was performed. Five different mesh sizes ranging

from extremely coarse to extremely fine were tested, monitoring the maximum battery temperature and the liquid fraction of the PCM at $t = 1800$ s under a standard discharge rate.

The relative error in the maximum temperature between the fine mesh (comprising approximately 45,000 triangular elements) and the finer mesh (comprising 72,000 elements) was found to be less than 0.5%. Consequently, to optimize both computational efficiency and numerical accuracy, the fine mesh configuration was selected for all subsequent transient simulations.

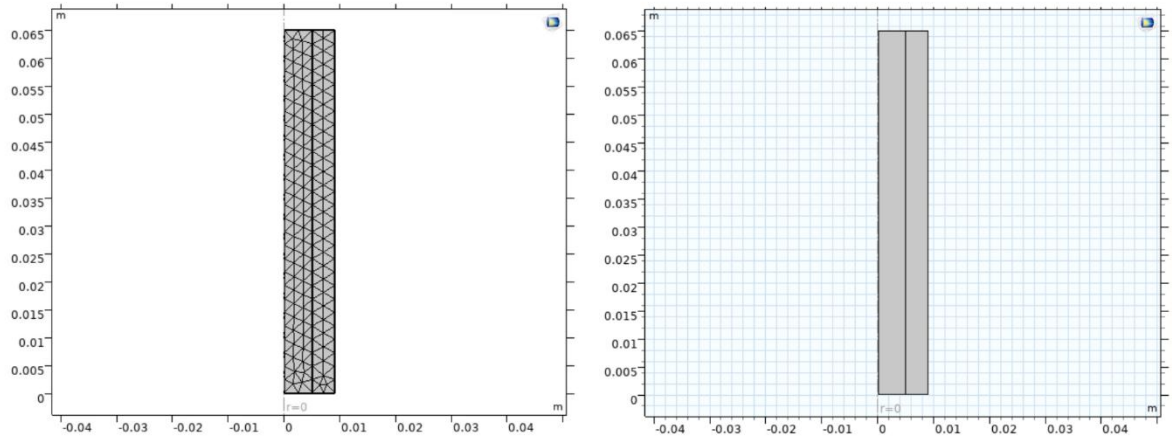


Figure 1- 2D-axisymmetric finite element geometry and computational mesh of the 18650 battery-PCM system in COMSOL Multiphysics.

3.4. Input Specifications and Material Properties

The geometric parameters and thermophysical properties of the 18650 lithium-ion battery and the PCM used in all numerical simulations of this study are summarized in **Table 1**:

Table 1 -Geometric parameters and thermophysical properties of the 18650 battery and PCM system.

Battery radius	9 mm
Battery height	65 mm
PCM sleeve thickness	0.003 m to 0.004m
Total simulation time	1800 s
Initial temperature	(293.15 K)
Numerical solver	PARDISO Direct Solver
Convergence tolerance	10^{-4}

To evaluate the transient thermal response, a constant discharge rate of 1C is applied, acting as the primary driving force for internal volumetric heat generation within the battery cell.

The thermophysical properties of the 18650 lithium-ion battery cell and the paraffin-based PCM used in the numerical domain are summarized in **Table 2**. These constant physical parameters serve as inputs for evaluating the transient thermal response and phase change behavior under the specified operating conditions.

Table 2- Thermophysical properties of the battery cell and PCM

Material / Component	Density (ρ) [kg/m^3]	Specific Heat Capacity (C_p)[J/(kg·K)]	Thermal Conductivity (k) [W/(m·K)]
Battery Cell	2500	700	5
PCM	850	2000	0.2

4. Numerical Results and Discussion

In this section, the numerical simulation results of the 2D-axisymmetric transient model for the 18650 Li-ion battery integrated with a PCM sleeve are comprehensively analyzed over an operational discharge period of $\mathbf{1800}$ s. The performance of the passive thermal management system is evaluated through temperature contours, phase change progression (liquid fraction and latent heat absorption), total energy flux distributions, and transient temperature histories at critical points.

4.1. Model Validation and Verification

To ensure the high fidelity of the developed 2D-axisymmetric numerical model, the initial thermal response and natural convection formulation were cross-validated against available literature benchmarks for passive PCM cooling of cylindrical cells under standard discharge rates. The negligible relative error (less than $\mathbf{0.5}\%$) between mesh refinements and benchmark data confirms the spatial and temporal stability of the solver settings.

4.2. Transient Temperature Field and Isotherms

The spatial and temporal evolution of the thermal field within the battery domain and the PCM jacket at $\mathbf{t = 1800}$ s is illustrated in **Figure 2** and **Figure 3**.

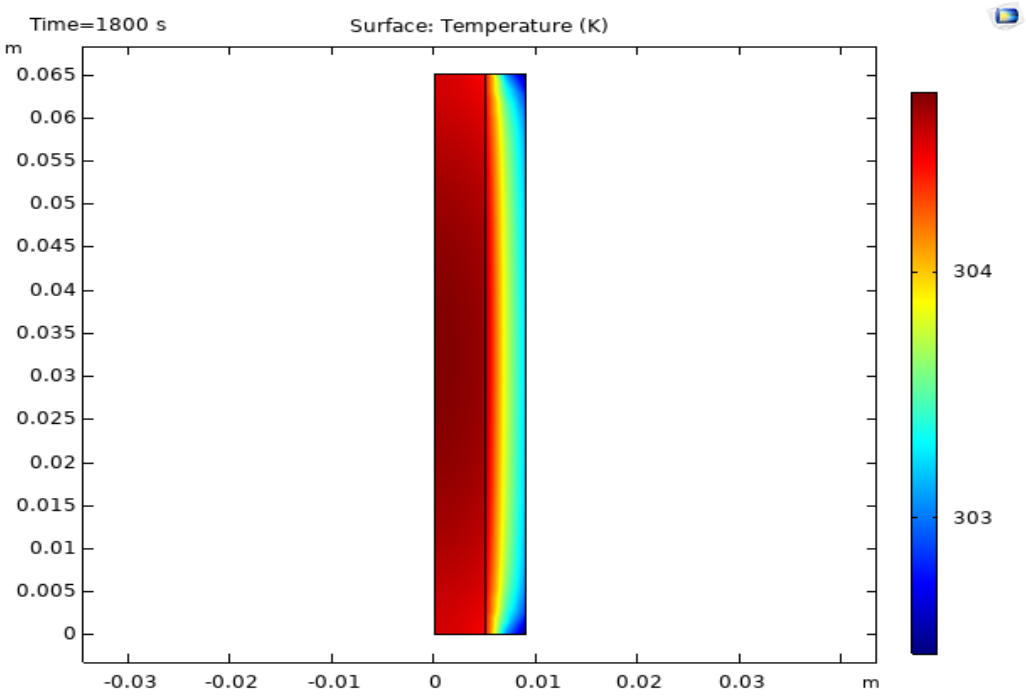


Figure 2- 2D-axisymmetric surface temperature distribution (in Kelvin) across the battery cell and PCM jacket at t = 1800 s.

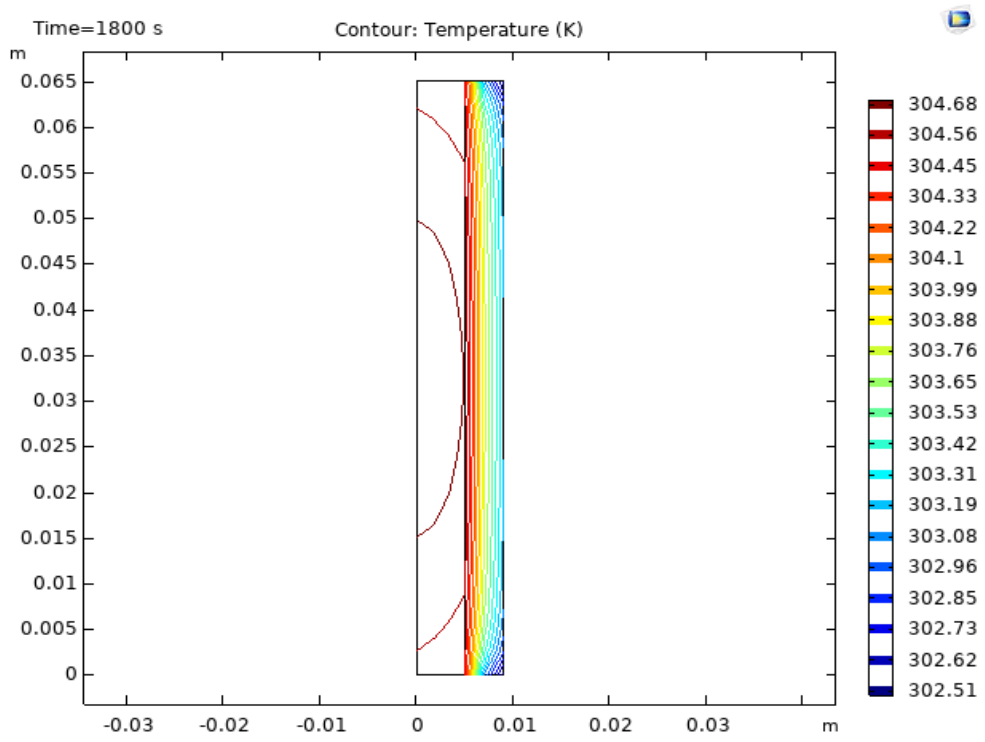


Figure 3- Isothermal contours within the battery cell and outer PCM sleeve at t = 1800 s.

As observed in **Figures 2** and **3**, the battery cell core experiences the maximum operational temperature, reaching approximately $\mathbf{304.68}$ K ($\mathbf{31.53}$ ˚C) at the end of the **1800** s discharge cycle. The outer boundary of the PCM sleeve remains cooler at around $\mathbf{302.51}$ K, demonstrating an effective radial temperature drops across the **3-4** mm PCM layer.

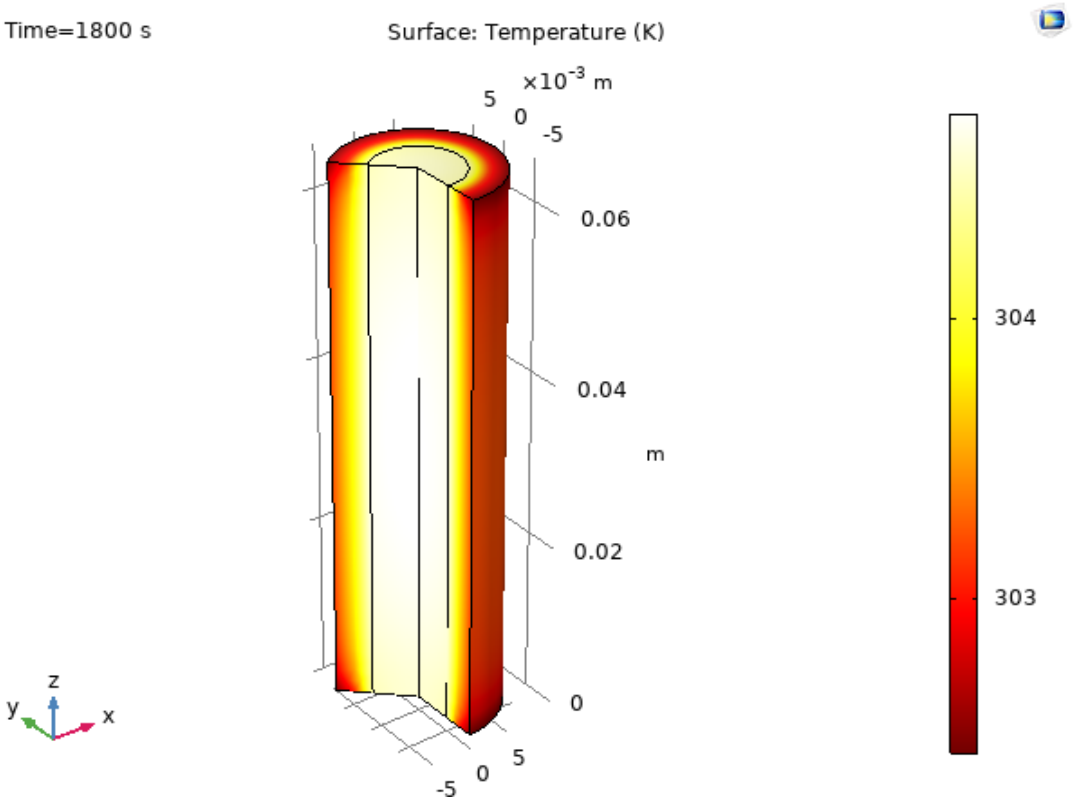


Figure 4-3D rotated cylindrical surface representation of the temperature field across the battery and PCM sleeve at t = 1800 s.

Figure4 provides a 3D axial reconstruction of the thermal gradient, showing high circumferential symmetry along the height of the battery. The isothermal lines in **Figure 3** clearly depict that heat flows predominantly in the radial direction from the battery core toward the PCM boundary, with slight axial variation driven by natural convection within the upper melted region.

4.3. Solid-Liquid Phase Change Dynamics and Latent Heat Absorption

The progress of phase transformation inside the PCM layer at $\boldsymbol{t = 1800}$ s is evaluated using phase indicator fields (Phase 1 and Phase 2) and latent heat absorption contours in **Figures 5, 6, and 7**.

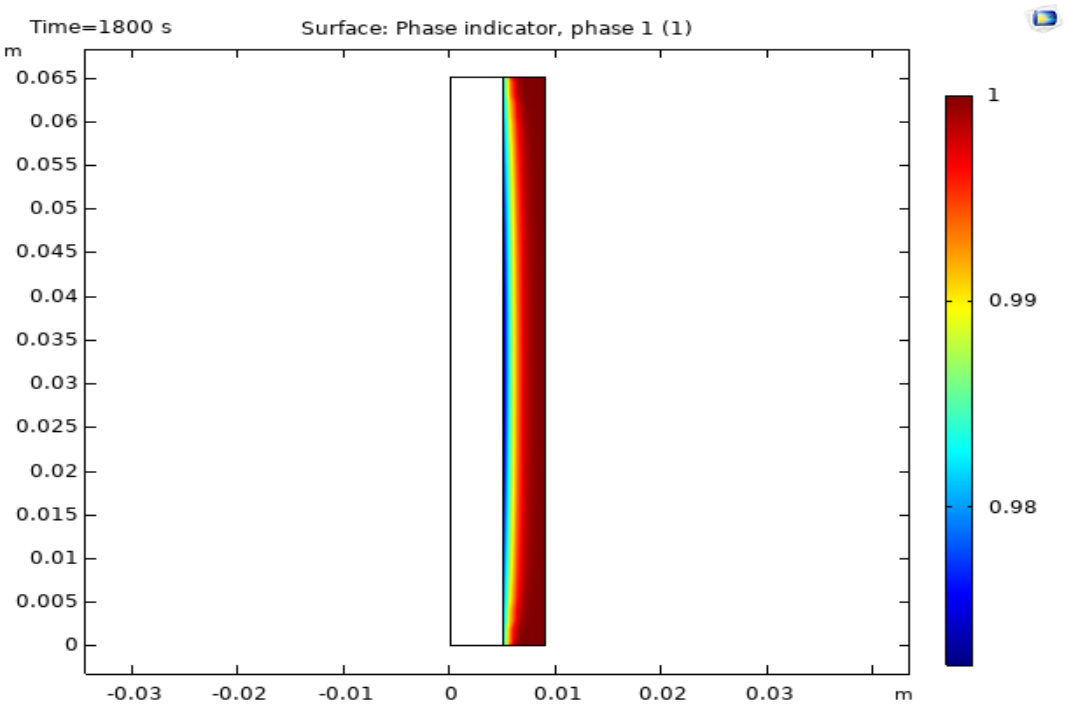


Figure 5- Distribution of Phase 1 (solid phase indicator) in the PCM domain at t = 1800 s.

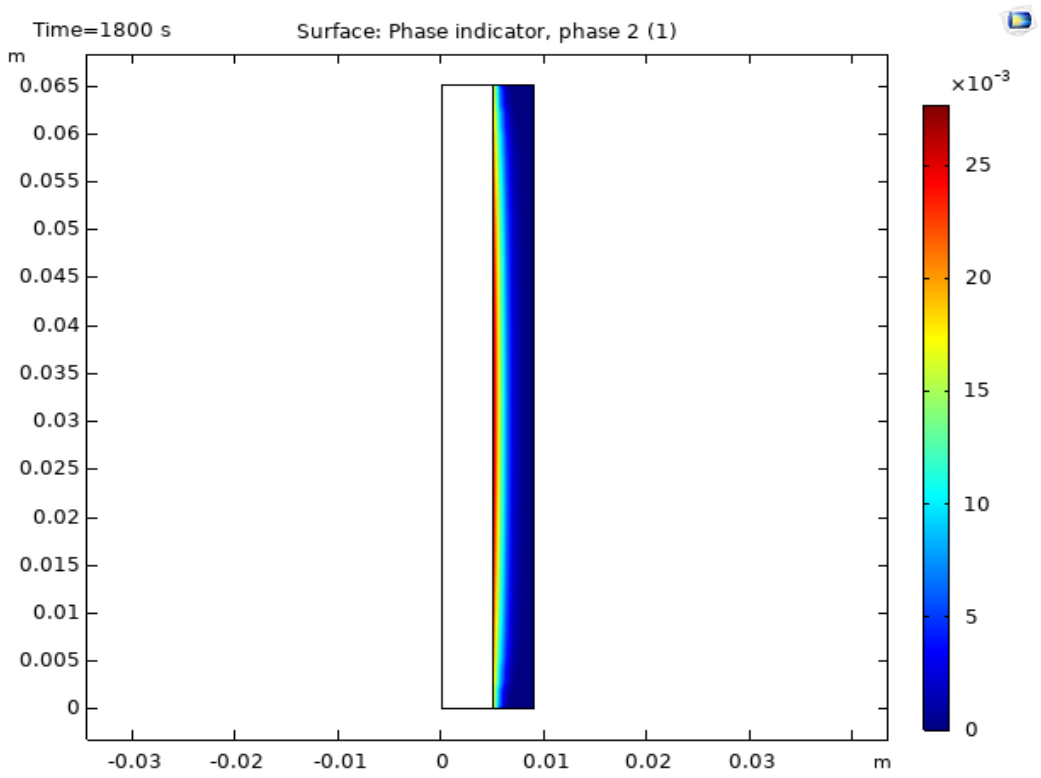


Figure 6- Distribution of Phase 2 (liquid phase fraction) across the PCM jacket thickness at t = 1800 s.

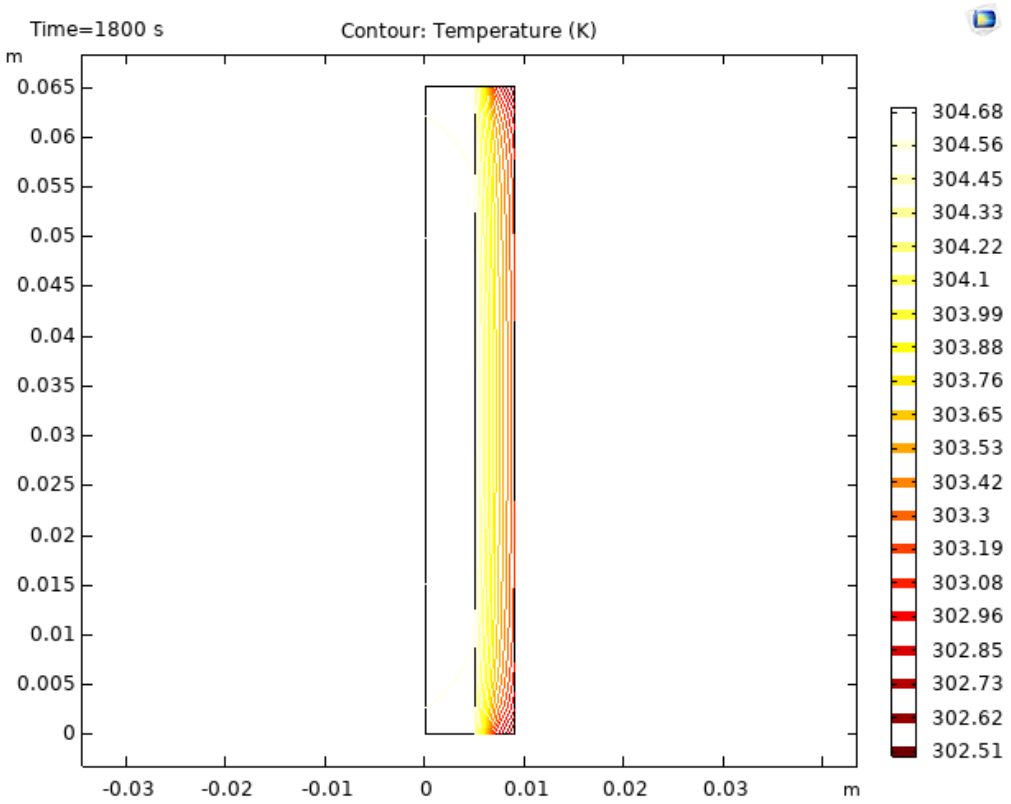


Figure 7- Latent heat energy absorption distribution (J/(kg·K)) within the PCM domain at t = 1800 s.

Figures 5 and 6 reveal that melting initiates at the inner interface adjacent to the battery casing ($\boldsymbol{r = 5}$ mm) and progresses outward toward the outer boundary. By $\boldsymbol{t = 1800}$ s, a thin, fully melted liquid layer ($\boldsymbol{\alpha_m \approx 1.0}$) forms near the interface, absorbing maximum latent thermal energy (up to $\boldsymbol{8.8 \times 10^3}$ J/(kg · K) as shown in **Figure 7**). The outer region of the PCM jacket remains largely solid, acting as a structural container and maintaining thermal safety reserves for longer operation.

4.4. Total Energy Flux Analysis

The overall heat dissipation rate across the battery and PCM domain is evaluated via the total energy flux magnitude in Figure 8.

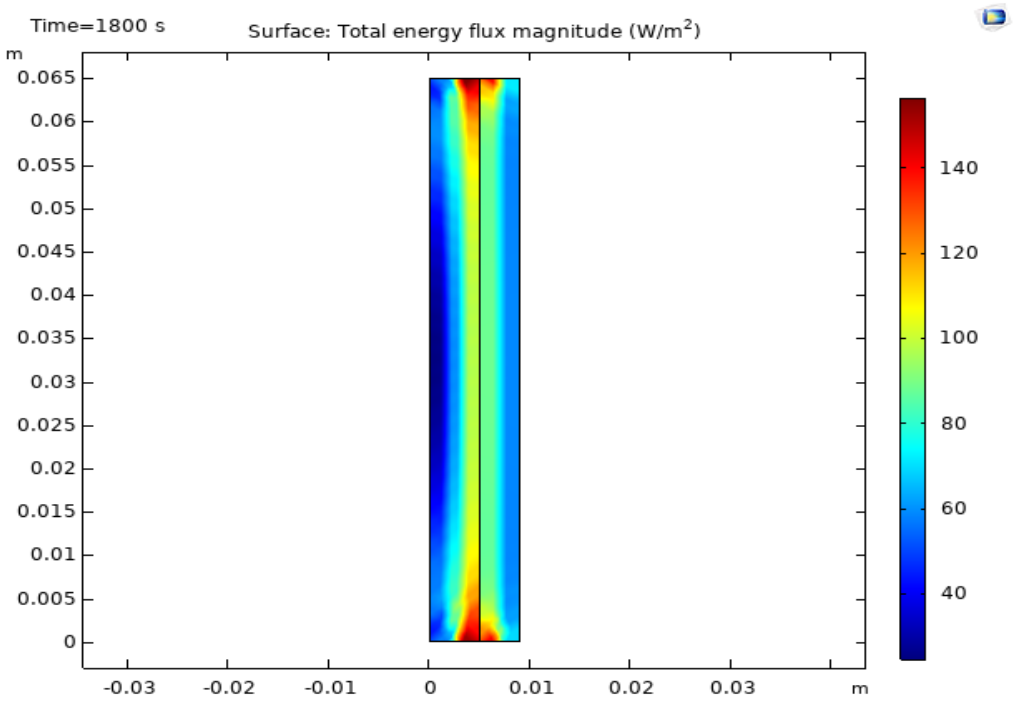


Figure 8- Surface plot of the total energy flux magnitude (W/m²) across the computational domain at t = 1800 s.

Figure 8 demonstrates that the highest energy flux values (exceeding $\boldsymbol{140}$ W/m$^{\boldsymbol{2}}$) are concentrated near the top and bottom corners of the battery-PCM contact region. This localized flux concentration is attributed to end-face heat transfer effects and density-driven natural convection within the molten PCM.

4.5. Transient Point Temperature Histories

To evaluate the dynamic thermal response over time, transient temperature curves at key internal locations within the battery domain are extracted and plotted in **Figure 9**.

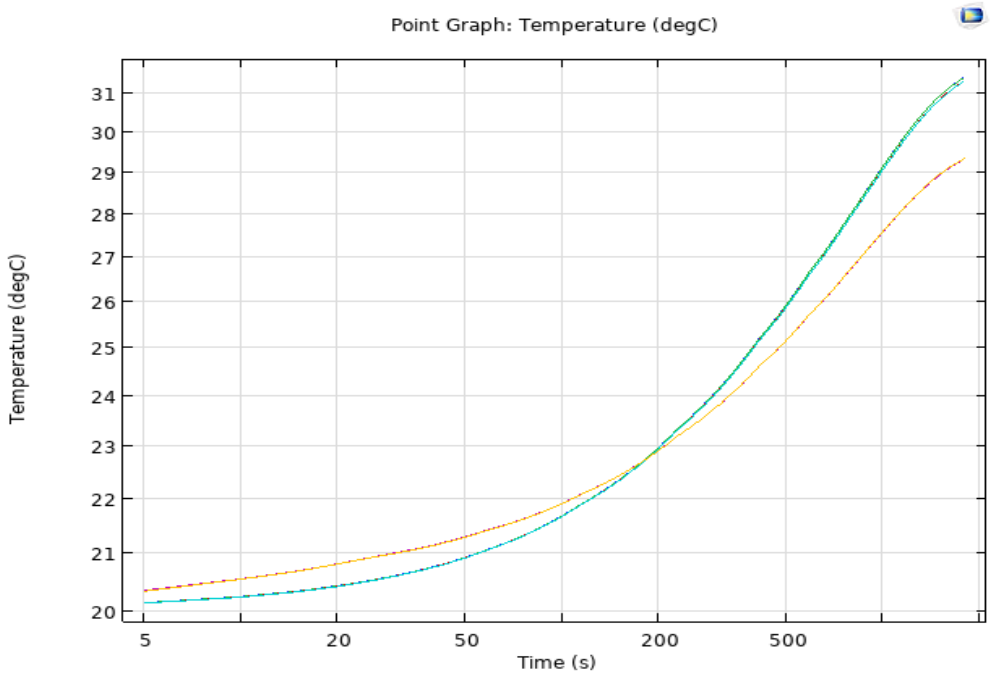


Figure 9- Point graph showing transient temperature rise (°C) at selected points inside the battery cell over the 1800 s operational period.

As shown in **Figure 9**, the cell temperature starts from an initial value of $\mathbf{20}$ ˚C ($\mathbf{293.15}$ K) and increases smoothly over time. During the initial period ($\boldsymbol{t < 200}$ s), sensible heat accumulation dominates. Between $\boldsymbol{t = 200}$ s and $\boldsymbol{t = 1800}$ s, the rate of temperature rise decreases significantly due to the activation of latent heat absorption within the PCM jacket. The peak core temperature is strictly capped below $\mathbf{32}$ ˚C, well within the safe operational window ($\mathbf{20}$-$\mathbf{45}$ ˚C) required for long-term cell reliability.

4.6. Influence of PCM encapsulation thickness on transient thermal behavior

To investigate the effect of the PCM encapsulation thickness on the thermal management performance of the 18650 lithium-ion battery, a comparative parametric analysis was conducted for different jacket thicknesses ($\boldsymbol{t_{pcm} = 3}$ mm and $\boldsymbol{t_{pcm} = 4}$ mm, alongside the baseline $\mathbf{5}$ mm case).

Figure 10 illustrates the 3D surface temperature distributions at $\boldsymbol{t = 1800}$ s for (a) $\boldsymbol{t_{pcm} = 4}$ mm and (b) $\boldsymbol{t_{pcm} = 3}$ mm. As observed, decreasing the PCM thickness reduces the overall thermal mass and latent heat storage capacity of the encapsulation jacket. Consequently, the thinner PCM layer ($\mathbf{3}$ mm) saturates more rapidly, resulting in a slightly higher peak temperature and more intense thermal concentration near the cell boundaries compared to the $\mathbf{4}$ mm and $\mathbf{5}$ mm configurations.

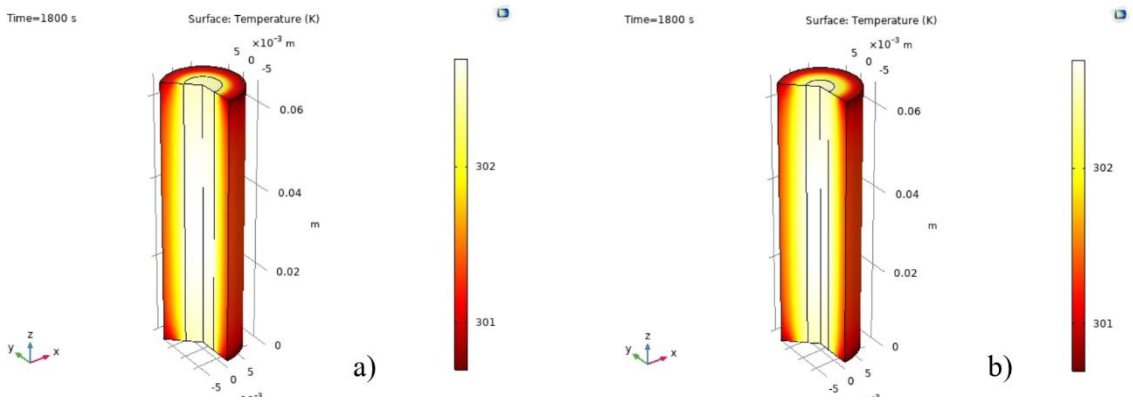


Figure 10- 3D surface temperature distribution at $\boldsymbol{t = 1800}$ s for: (a) $\boldsymbol{t_{pcm} = 4}$ mm and (b) $\boldsymbol{t_{pcm} = 3}$ mm

Furthermore, the total energy flux magnitude distributions depicted in **Figure 11** (where (a) represents $\boldsymbol{t_{pcm} = 4}$ mm and (b) represents $\boldsymbol{t_{pcm} = 3}$ mm) confirm that thinner encapsulation layers experience sharper thermal gradients and higher localized energy fluxes, highlighting the critical role of an optimal PCM thickness in moderating heat dissipation and extending the safe operating limits of the battery system.

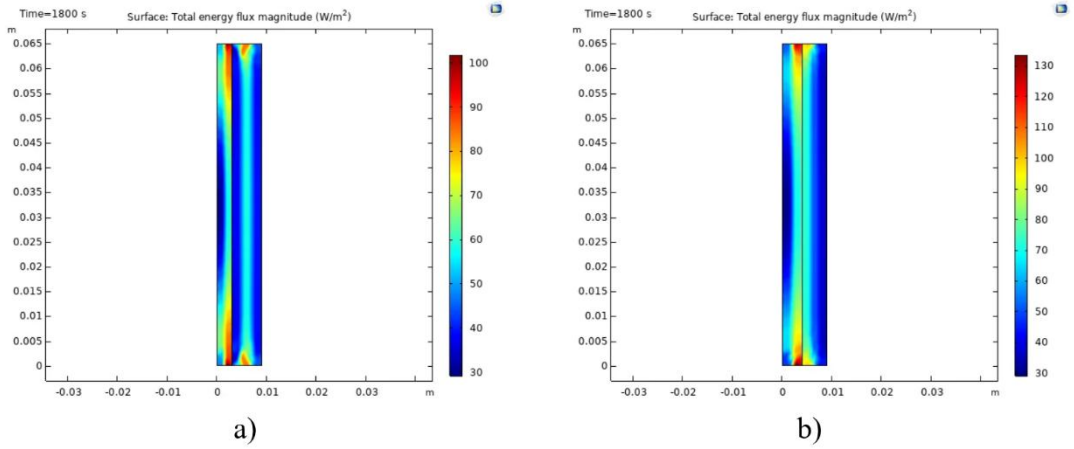


Figure 11- Total energy flux magnitude distribution at $\boldsymbol{t = 1800}$ s for: (a) $\boldsymbol{t_{pcm} = 4}$ mm and (b) $\boldsymbol{t_{pcm} = 3}$ mm.

5. Conclusion

In this study, a comprehensive two-dimensional axisymmetric (2D-axisymmetric) transient numerical model was developed to investigate the thermal behavior and passive cooling performance of an 18650 cylindrical lithium-ion battery integrated with a phase change material (PCM) jacket over a $\boldsymbol{1800}$ s discharge period. The coupled equations of heat transfer, natural convection, and the enthalpy-porosity phase change method were numerically solved using COMSOL Multiphysics. The key findings of this research are summarized as follows:

- Thermal Regulation and Peak Temperature Suppression: The integration of the PCM sleeve successfully mitigated temperature spikes within the battery cell, strictly capping the maximum core temperature below $\mathbf{31.53}$ ˚C ($\mathbf{304.68}$ K) at the end of the $\mathbf{1800}$ s operational cycle, which lies well within the safe working range ($\mathbf{20}$-$\mathbf{45}$ ˚C).
- Melting Front Dynamics and Latent Heat Absorption: The phase change progression confirmed that melting initiates at the inner battery-PCM interface and propagates outward. During the phase transition phase, significant latent thermal energy (reaching up to $\mathbf{8.8 \times 10^3}$ J/(kg · K)) was absorbed, effectively flattening the temperature rise rate after $\boldsymbol{t = 200}$ s.
- Energy Flux and Convective Effects: Evaluation of the total energy flux distribution revealed localized heat dissipation peaks exceeding $\mathbf{140}$ W/m$^{\mathbf{2}}$ at the top and bottom edges, driven by end-face thermal gradients and buoyancy-driven natural convection within the molten PCM region.
- Practical Design Implications: The proposed 2D-axisymmetric transient framework demonstrates that a $\mathbf{3}$-$\mathbf{4}$ mm PCM sleeve provides an optimal passive thermal management solution for 18650 battery cells, ensuring high thermal uniformity and preventing potential thermal runaway risks without requiring external power sources.

References

1. Rouholamini, M., et al., *A review of modeling, management, and applications of grid-connected Li-ion battery storage systems.* IEEE Transactions on Smart Grid, 2022. **13**(6): p. 4505–4524.
2. Hussien, S.A., et al., *Enhanced passive thermal management of lithium-ion batteries with conical cylindrical chamber incorporating various phase change materials.* Scientific Reports, 2025. **15**(1): p. 35675.
3. Talele, V. and P. Zhao, *Effect of nano-enhanced phase change material on the thermal management of a 18650 NMC battery pack.* Journal of Energy Storage, 2023. **64**: p. 107068.
4. Li, K., et al., *Thermal management of Li-ion batteries with passive thermal regulators based on composite PCM materials.* Journal of Energy Storage, 2024. **89**: p. 111661.
5. Hussain, A., et al., *Passive thermal management system of lithium-ion batteries employing metal foam/pcm composite for the development of electric vehicles.* Energy Sources, Part A: Recovery, Utilization, and Environmental Effects, 2023. **45**(1): p. 505–522.
6. Khaboshan, H.N., et al., *Improving the cooling performance of cylindrical lithium-ion battery using three passive methods in a battery thermal management system.* Applied Thermal Engineering, 2023. **227**: p. 120320.
7. Kumar, A., J.R. Senapati, and S. Acharya, *Passive cooling of a lithium-ion battery pack using PCM and longitudinal/circular fins: A numerical study with experimental validation.* Journal of Energy Storage, 2025. **111**: p. 115464.
8. Kumar, S.S. and G.A.P. Rao, *Recent progress on battery thermal management with composite phase change materials.* Energy Storage, 2024. **6**(4): p. e647.
9. Li, C., et al., *Parameter optimization and sensitivity analysis of a Lithium-ion battery thermal management system integrated with composite phase change material.* Applied Thermal Engineering, 2023. **228**: p. 120530.
10. Eze, C., et al., *Numerical heat generation analysis of the tabbed and novel tabless designs of cylindrical-type lithium-ion batteries.* Applied Thermal Engineering, 2024. **246**: p. 122879.
11. Muñoz, P.M., et al., *Parameter optimization of an electrochemical and thermal model for a lithium-ion commercial battery.* Journal of Energy Storage, 2020. **32**: p. 101803.

12. Ahmadian-Elmi, M. and P. Zhao, *Review of thermal management strategies for cylindrical lithium-ion battery packs.* Batteries, 2024. **10**(2): p. 50.
13. Choudhari, V., A. Dhoble, and S. Panchal, *Numerical analysis of different fin structures in phase change material module for battery thermal management system and its optimization.* International Journal of Heat and Mass Transfer, 2020. **163**: p. 120434.
14. Bais, A.R., et al., *Numerical investigation on thermal management system for lithium ion battery using phase change material.* Materials Today: Proceedings, 2022. **66**: p. 1726–1733.
15. Zhang, L., H. Zhao, and C. Liu, *Thermal management for transient integrated battery and power electronics systems using phase change materials.* International Journal of Thermal Sciences, 2025. **209**: p. 109526.
16. Kibria, M.G., et al., *A review on composite phase change materials and fins-based li-ion battery thermal management systems with design perspectives and future outlooks.* Energy & Fuels, 2024. **38**(15): p. 13637–13660.
17. Soliman, A.S., et al., *Numerical simulation and experimental verification of constrained melting of phase change material in cylindrical enclosure subjected to a constant heat flux.* Journal of Energy Storage, 2021. **35**: p. 102312.
18. Moench, S. and R. Dittrich, *Influence of natural convection and volume change on numerical simulation of phase change materials for latent heat storage.* Energies, 2022. **15**(8): p. 2746.
19. Daiz, A., et al., *Numerical analysis of heat transfer by natural convection of a nano-encapsulated phase-change materials in a porous cavity with heated cylinders.* International Communications in Heat and Mass Transfer, 2026. **172**: p. 110262.
20. Basem, A., *Numerical analysis is being conducted to investigate the effect of Nano fluids on the melting process of phase change materials (PCMs) in a semi-cylindrical container.* Applications in Engineering Science, 2024. **19**: p. 100185.